JOURNAL OF BACTERIOLOGY, June 1999, p. 3330–3340 Vol. 181, No. 11
0021-9193/99/$04.00+0

Saccharomyces cerevisiae Mid2p Is a Potential Cell Wall Stress Sensor and Upstream Activator of the *PKC1-MPK1* Cell Integrity Pathway

TROY KETELA, ROBIN GREEN, AND HOWARD BUSSEY*

Department of Biology, McGill University, Montreal, Quebec, Canada H3A 1B1

Received 20 January 1999/Accepted 15 March 1999

The *MID2* gene of *Saccharomyces cerevisiae* encodes a protein with structural features indicative of a plasma membrane-associated cell wall sensor. *MID2* was isolated as a multicopy activator of the Skn7p transcription factor. Deletion of *MID2* causes resistance to calcofluor white, diminished production of stress-induced cell wall chitin under a variety of conditions, and changes in growth rate and viability in a number of different cell wall biosynthesis mutants. Overexpression of *MID2* causes hyperaccumulation of chitin and increased sensitivity to calcofluor white. α-Factor hypersensitivity of *mid2*Δ mutants can be suppressed by overexpression of upstream elements of the cell integrity pathway, including *PKC1*, *RHO1*, *WSC1*, and *WSC2*. Mid2p and Wsc1p appear to have overlapping roles in maintaining cell integrity since *mid2*Δ *wsc1*Δ mutants are inviable on medium that does not contain osmotic support. A role for *MID2* in the cell integrity pathway is further supported by the finding that *MID2* is required for induction of Mpk1p tyrosine phosphorylation during exposure to α-factor, calcofluor white, or high temperature. Our data are consistent with a role for Mid2p in sensing cell wall stress and in activation of a response that includes both increased chitin synthesis and the Mpk1p mitogen-activated protein kinase cell integrity pathway. In addition, we have identified an open reading frame, *MTL1*, which encodes a protein with both structural and functional similarity to Mid2p.

The cell wall is an essential organelle in fungal species. In *Saccharomyces cerevisiae* it is composed of four polysaccharide polymer classes: β-1,3-glucan, β-1,6-glucan, mannan, and chitin. The functions provided by the yeast cell wall include the determination of cell shape, protection of osmotic integrity, and scaffolding for extracellular proteins important for nutrient uptake and agglutination between mating partners. Recent research has emphasized the dynamic nature of this structure (see references 10 and 37 for reviews), which undergoes major changes in shape and composition during the vegetative budding cycle and the alternative developmental pathways of mating and sporulation.

Stress can lead to alteration of polymer levels in the yeast cell wall. This effect is perhaps best documented for chitin. Schekman and Brawley (44) noted that during shmoo formation, a process during which the cell wall is rapidly remodeled, additional chitin is synthesized and deposited at the base and neck region of the mating projection. Roncero and Duran (43) noted that exposure to calcofluor white, a substance which binds primarily chitin in the yeast cell wall, interferes with proper wall synthesis and induces elevated chitin synthesis in vivo. Recently, Popolo et al. (39) and Ram et al. (41) observed that mutational disruption of cell wall biosynthesis caused increased chitin deposition. This finding led to the proposal that alterations in cell wall assembly cause yeast to engage a compensation mechanism that includes increased chitin synthesis.

The *PKC1-MPK1* signal transduction pathway plays an essential role in maintaining the integrity of the cell wall during both mating and vegetative growth. Igual et al. (20) showed that at least part of this influence on cell wall construction is the result of control of transcription of a variety of genes involved in cell wall biosynthesis. Pkc1p, a serine/threonine protein kinase (28), serves to stimulate a mitogen-activated protein (MAP) kinase cascade comprised of Bck1p (Slk1p) (11, 26, 29), Mkk1p/Mkk2p (21), and Mpk1p (Slt2p) (27). Mutation of components in the *PKC1-MPK1* pathway have a range of effects, such as cell lysis, caffeine sensitivity, cell cycle progression defects, and defective cytoskeletal organization. The molecular basis of yeast Pkc1p stimulation is not yet fully understood; however, the GTP-bound form of the small G-protein, Rho1p, has been shown to physically associate with Pkc1p, resulting in Pkc1p activation (14, 24, 35).

Studies of the extracellular matrix of mammalian cells, a structure analogous to the yeast cell wall, have revealed a class of protein receptors known as integrins. Integrins possess a large extracellular domain, a single membrane-spanning region, and a short cytoplasmic domain. Activation of protein kinases and small GTP-binding proteins such as RhoAp by integrins affects cell adhesion, cellular ion levels, and polarized growth. Recently, Bickle et al. (3) have proposed that disturbances in the cell wall cause activation of the Rho1p GTPase via the Rom2p exchange factor in a manner analogous to integrin signaling. Although the proteome of *S. cerevisiae* does not include integrin homologs, there are a number of cell surface proteins topologically resembling integrins that could potentially carry out equivalent extracellular sensing/intracellular signaling processes. These proteins, usually type I in orientation, contain large extracellular regions rich in serine and threonine residues, single transmembrane domains, and relatively small cytoplasmic regions.

WSC1 (*HCS77*/*SLG1*) encodes a protein with sensor/signaler-like characteristics that has recently been identified as an upstream activator of Pkc1p (19, 22, 47). Three homologous proteins, encoded by the *WSC2*, *WSC3*, and *WSC4* genes, appear to have overlapping activity with Wsc1p since their deletion can increase the severity of *wsc1*Δ phenotypes (47). *wsc*Δ mutants display characteristics of cells with decreased Pkc1p

* Corresponding author. Mailing address: Department of Biology, McGill University, 1205 Dr. Penfield Ave., Montreal, Quebec, Canada H3A 1B1. Phone: 1-514-398-6439. Fax: 1-514-398-8051. E-mail: hbussey@monod.biol.mcgill.ca.

TABLE 1. Oligonucleotide sequences

Name	Sequence 5′-3′[a]
mid2Δup	GCAGTATCTACTGCACGTTCTTCCGTAAGTAGAGTTAGTTCT**GATATCAAGCTTGCCTCG**
mid2Δdown	TGTTTGGCGTTTGGTAATACGCTATCGCTATCTCTTATTCTG**GTCGACACTGGATGGCGG**
mid2Δtest	GCCTTCAATGAGTTCCAC
KANMX2 internal	**CAACAGGCCAGCCATTAC**
wsc1Δup	ATGAGACCGAACAAAACAAGTCTGCTTCTGGCGTTATTATCC**GATATCAAGCTTGCCTCG**
wsc1Δdown	TGGATTGACCACTGTTAAAACGTTGTTTTTCCCTCCTGGTCC**GTCGACACTGGATGGCGG**
wsc1Δtest	CGATACAGTAAACTCGAC
HA-insert	GAATTATCACCACGAAATTATTACCCATACGACGTCCCAGACTACGCTTAATCATATCCATTCATATC
EcoRI Insert	GCAATAAATCCAAGAATTCGGGTCTTTC
KpnI Insert	GGTAACGAATTATCACCACGAAAGGTACCATCATATCCATTCATATCATTTAG
rho1Δup	ATGTCACAACAAGTTGGTAACAGTATCAGAAGAAAGCTGGTAATC**ATGAGTAAAGGAGAAGAAC**
rho1Δdown	CTATAACAAGACACACTTCTTCTTCTTCTTTTCAGTAGTGTTCTT**GCGCGCCTCGTTCAGAATG**
rho1Δtest	CGACCATCGATCATTCCT
rho1 clone for	TAATGCGGTAGCATTGGACA
rho1 clone rev	AACCTTCCAACAAAACTGAGG
pkc1Δup	ATGAGTTTTTCACAATTGGAGCAGAACATTAAAAAAAAGATAGCC**ATGAGTAAAGGAGAAGAAC**
pkc1Δdown	TCATAAATCCAAATCATCTGGCATAAAGGAAAATCCTCTAAACTC**GCGCGCCTCGTTCAGAATG**
pkc1Δtest	CCTGCCAGTGTAATAAGT
GFP-HIS3 internal	**GTATAGTTCATCCATGCC**
mtl1 clone rev	CTTGCCTTCTCCAGAGG
mtl1 clone for prom.	CCACATCAGAGACTTGGG
mtl1 clone for start	GGTTGGTTCGATCTTCGT
mtl1Δup	CGGGTTGGTTCGATCTTCGTTTCCACTTTTAACTTACTCCC**ATGAGTAAAGGAGAAGAAC**
mtl1Δdown	GGGTGATTTTAAGAAGAAAAGTTATGGCAAAGCTGCTTTCG**GCGCGCCTCGTTCAGAATG**
mtl1Δtest	GGTAGAAAAGTGTAGATG

[a] Sequences internal to the *KANMX2* and *GFP-HIS3* cassettes are in boldface.

activity, namely, reduced growth rate and sorbitol-suppressible, temperature-dependent cell lysis. Overexpression of genes presumably downstream of the *WSC* family, such as *RHO1* and *PKC1*, can suppress some of the effects of *WSC* gene deletions. The mechanism by which Wsc proteins stimulate Pkc1p activity is not yet known, but it has been suggested that Wsc1p might somehow regulate Rho1p activity and thereby affect downstream targets of Rho1p such as Pkc1p (2).

Mid2p, although not a member of the *WSC* family, is another potential extracellular sensor that has been identified as a participant in a number of cellular processes. In wild-type *MAT***a** cells, transcription of *MID2* increases severalfold in response to α-factor and cells lacking Mid2p die during exposure to α-factor (36). Multicopy *MID2* has been found to suppress a variety of mutant phenotypes, including the temperature sensitivity of *mpt5*Δ mutants (46), growth in profilin (*pfy1*Δ)-deficient cells (32), and temperature-sensitive growth in *cik1*Δ and *kar3*Δ mutants (31). Additionally, *KAI1*, an internal fragment of *MID2* was identified as a multicopy inhibitor of excessive protein kinase A (*TPK1*) activity (12).

We identified *MID2* as a high-copy-number activator of the Skn7p transcription factor. A relationship between Mid2p and the cell wall is suggested by a number of genetic interactions between *MID2* and cell wall biosynthesis genes. Alteration of *MID2* gene dosage affects stress-related cell wall chitin deposition, suggesting that *MID2* is partly required for induction of cell wall stress-induced chitin synthesis. Furthermore, genetic interactions between *MID2* and elements of the *PKC1-MPK1* pathway, as well as a requirement for *MID2* during induction of Mpk1p tyrosine phosphorylation under a variety of stress conditions, together suggest a role for Mid2p upstream of the *PKC1-MPK1* cell wall integrity pathway.

MATERIALS AND METHODS

Plasmids, strains, and gene deletion constructs. Oligonucleotides used in this study are listed in Table 1. Yeast strains used in this study are listed in Table 2. The *MID2* locus, contained within a 2.45-kb *Nhe*I-*Xho*I genomic DNA fragment, was subcloned into pBluescript II (pBSII) SK+ at compatible *Xba*I and *Sal*I restriction sites. A 2.5-kb *Kpn*I-*Sst*I fragment containing *MID2* was excised from this plasmid and then inserted into pRS316, pRS425, and pRS426 at corresponding *Kpn*I-*Sst*I sites in the polylinker. Deletion of the entire *MID2* open reading frame (ORF) was accomplished by integration of a *mid2Δ::KANMX2* cassette (48). *mid2Δ::KANMX2* was generated by using the oligonucleotides *mid2Δup* and *mid2Δdown*. Correct insertion of the cassette and deletion of the reading

TABLE 2. Strains used

Strain	Genotype
L40	*MAT***a** *his3 trp1 leu2 ade2 LYS2::*$(lexAop)_4$*-HIS3 URA3::*$(lexAop)_8$*-lacZ GAL4*)
TK60	L40/pBTM116-*LEXA-SKN7*/pRS425
TK61	L40/pBTM116-*LEXA-SKN7*/pRS425-*MID2*
SEY6210[2]	*MAT*α/*MAT***a** *leu2/leu2 ura3/ura3 his3/his3 lys2/lys2 trp1/trp1 suc2/suc2*
SEY6210	*MAT*α *leu2 ura3 his3 lys2 trp1 suc2*
SEY6210a	*MAT***a** *leu2 ura3 his3 lys2 trp1 suc2*
TK82	SEY6210**a**/pRS426
TK83	SEY6210**a**/pRS426-*MID2*
TK84	SEY6210**a**/pRS426-*MID2-HA*
TK85	SEY6210**a**/pRS426-Δ*S/T-MID2-HA*
TK86	SEY6210**a**/pVT101U
TK87	SEY6210**a**/pVT101U-*MID2*
TK88	SEY6210**a** *mid2Δ::KANMX2*
TK89	SEY6210**a** *mid2Δ::KANMX2*/pRS425
TK90	SEY6210**a** *mid2Δ::KANMX2*/pRS425-*WSC1*
TK91	SEY6210**a** *mid2Δ::KANMX2*/pRS425-*WSC2*
TK92	SEY6210**a** *mid2Δ::KANMX2*/pRS425-*RHO1*
TK93	SEY6210**a** *mid2Δ::KANMX2*/pFL44
TK94	SEY6210**a** *mid2Δ::KANMX2*/pFL44-*MPK1-HA*
TK95	SEY6210**a**/pRS425
TK96	SEY6210**a**/pFL44
TK97	SEY6210**a**/pFL44-*MPK1-HA*
TK98	SEY6210**a**/pRS426-*MID2-GFP*
TK99	SEY6210**a** *chs3Δ::LEU2*/pVT101U
TK100	SEY6210**a** *chs3Δ::LEU2*/pVT101U-*MID2*
TK101	SEY6210[2] *kre6Δ::HIS3/KRE6 mid2Δ::KANMX2/MID2*
TK102	SEY6210[2] *kre9Δ::HIS3/KRE9 mid2Δ::KANMX2/MID2*
TK103	SEY6210[2] *fks1Δ::HIS3/FKS1 mid2Δ::KANMX2/MID2*
TK104	SEY6210[2] *wsc1Δ::KANMX2 mid2Δ::KANMX2/MID2*
TK105	SEY6210[2] *mtl1Δ::GFP-HIS3 mid2Δ::KANMX2/MID2*

frame was confirmed by PCR analysis of yeast colonies using the oligonucleotides *mid2Δtest* and *KANMX2 internal*. Deletion of *WSC1* was accomplished by replacement of the *WSC1* reading frame with a *wsc1Δ::KANMX2* cassette generated by the oligonucleotides *wsc1Δup* and *wsc1Δdown*. Integration was confirmed by using the *KANMX2 internal* test oligonucleotide and the *wsc1Δtest* oligonucleotide. Deletion of *RHO1* was accomplished by using a *GFP-HIS3* cassette (34) and the oligonucleotides *rho1Δup* and *rho1Δdown* to create *rho1Δ::GFP-HIS3*. Correct integration of the deletion cassette into the SEY6210[2] (diploid) strain was confirmed by using the oligonucleotides *rho1Δtest* and *GFP-HIS3 internal*; 2:2 segregation of viable and inviable meiotic products was observed after dissection of tetrads derived from heterozygous *rho1::GFP-HIS3 RHO1* diploids. Deletion of *PKC1* was achieved by using the oligonucleotides *pkc1Δup* and *pkc1Δdown* to generate the *pkc1Δ::GFP-HIS3* cassette. Integration of the PCR product was confirmed by using the oligonucleotides *pkc1Δtest* and *GFP-HIS internal*. Deletion of *MTL1* was accomplished by replacement of the *MTL1* reading frame with a *mtl1Δ::GFP-HIS3* cassette generated by the nucleotides *mtl1Δup* and *mtl1Δdown*. Correct integration was confirmed by using the *GFP-HIS3 internal* and *mtl1Δtest* nucleotides.

The *RHO1* and *MTL1* genes were amplified from SEY6210 genomic DNA by using Expand polymerase (Boehringer Mannheim) and the oligonucleotides *rho1 clone for* and *rho1 clone rev* to generate *RHO1* and *mtl1 clone rev* and either *mtl1 clone for prom* or *mtl1 clone for start* to generate clones of *MTL1* containing 916 nucleotides of promoter sequence or a promoterless clone with only 65 nucleotides 5′ of the ATG codon, which was used for fusion to the *ADH1* promoter.

Mid2p-HA was created by the insertion of a single copy of the hemagglutinin (HA) epitope (YPYDVPDYA) between residues 375 and 376 via site-directed mutagenesis (Kunkel method [25]) on *MID2* contained in pBSII KS−, using the oligonucleotide *HA-insert*. Fidelity of incorporation of the HA epitope was confirmed by DNA sequencing. A *Kpn*I-*Sst*I fragment containing *MID2-HA* was then subcloned into pRS316 and pRS426 at corresponding *Kpn*I and *Sst*I sites. Mid2p-HA was demonstrated to be functional by the observation that pRS316-*MID2-HA* was fully able to complement a *mid2Δ* mutant in a test for hypersensitivity to α-factor (Sigma).

Removal of the serine/threonine-rich region was accomplished by generating an *Eco*RI restriction site by modification of the sequence AAGTTC (nucleotides 641 to 646 in the *MID2* reading frame) to GAATTC via site-directed mutagenesis using the oligonucleotide *EcoRI Insert*. A second *Eco*RI restriction site occurs naturally at positions 102 to 107 in the reading frame. This construct was then digested with *Eco*RI, releasing a 540-bp fragment coding for the bulk of the serine/threonine-rich region. The remaining plasmid fragment was gel purified (Pharmacia) and religated, creating the continuous in-frame ORF *ΔS/T-MID2*.

Western blots and membrane association tests. For membrane association tests, total cell extracts were prepared from mid-log-phase cultures grown in selective medium by vigorous vortexing in lysis buffer (50 mM Tris [pH 7.5], 1 mM EDTA, 5% glycerol) in the presence of glass beads and protease inhibitors (Complete protease inhibitor cocktail; Boehringer Mannheim). The resulting slurry was centrifuged at 2,500 × *g* at 4°C for 5 min to remove cell walls and unbroken cells. The resulting supernatant was then divided, and the individual aliquots were subjected to either centrifugation at 15,000 × *g* at 4°C for 30 min or treatment with sodium chloride, sodium carbonate, urea, or Triton X-100 and then subjected to centrifugation at 60,000 × *g* at 4°C for 30 min. Postcentrifugation, supernatants were withdrawn, and pellets were resuspended in a volume of lysis buffer equal to the supernatant. Samples were resolved by sodium dodecyl sulfate-polyacrylamide gel electrophoresis (SDS-PAGE) and then subjected to Western blotting. Immunodetection of Mid2p-HA was achieved by using anti-HA monoclonal antibody 12CA5 (Babco) at 1:1,000 dilution and horseradish peroxidase-conjugated anti-mouse secondary antibody (Amersham Life Sciences) at a 1:1,000. Bands were visualized using by enhanced chemiluminescence (Amersham Life Sciences). For other SDS-PAGE and Western blotting procedures, total cell lysates were prepared with lysis buffer (2% Triton-X100, 1% SDS, 100 mM NaCl, 10 mM Tris-HCl [pH 8.0], 1 mM EDTA).

Localization of Mid2p. A *MID2-GFP* fusion was generated by modifying the coding sequence of *MID2* (contained in pBSII KS−) immediately upstream of the TAA stop codon (TTATTA) via site-directed mutagenesis to a *Kpn*I restriction site (GGTACC), using the oligonucleotide *KpnI Insert*. Clones positive for the incorporation of the *Kpn*I site were then confirmed by sequencing. Creation of an in-frame fusion of *MID2* to *GFP* (F64L S65T; kindly provided by U. Stochaj) was accomplished by a three-way ligation involving pRS426 or pRS316 (with *Xho*I/*Eco*RI ends) *MID2* (with *Xho*I/*Kpn*I ends) and *GFP* (with *Kpn*I/*Eco*RI ends). Correct orientation of the ligation products was confirmed by diagnostic restriction digests. Function of the *MID2-GFP* fusion was demonstrated by observation that pRS316-*MID2-GFP* fully complements *mid2Δ* mutants for α-factor hypersensitivity. Localization of Mid2p-GFP (green fluorescent protein) was accomplished by examination of live, mid-log-phase *mid2Δ* cells carrying pRS316-*MID2-GFP* and pRS426-*MID2-GFP*.

Calcofluor white tests. To test strains for sensitivity to calcofluor white, mid-log-phase cells were diluted, then spotted either onto rich YEPD agar plates containing the indicated amount of calcofluor white or onto selective medium buffered with 10 g of morpholineethanesulfonic acid per liter and adjusted to pH 6.2. Plates were incubated for 48 to 72 h at 30°C in a dark environment.

Multicopy suppression of α-factor-induced death. Cultures of cells containing either control plasmids or plasmids bearing genes of interest were diluted to 3 × 10^4 cells/ml in buffered (85 mM succinic acid, 19 mM sodium hydroxide) YNB liquid medium containing appropriate amino acids. Triplicate aliquots of each strain were removed and spread on selective solid medium. α-Factor was then added to liquid cultures to a final concentration of 1 μM, and these cultures were incubated at 30°C for 330 min before a second series of aliquots were removed and plated. Petri dishes were incubated for 48 h at 30°C, resulting in the formation of colonies derived from single cells. The number of colonies on each petri dish was counted, and survival of α-factor exposure was measured by the difference between the number of colonies on pre- and post-α-factor petri dishes for each strain.

Chitin assays. Total cellular chitin was measured essentially as described by Bulawa et al. (9) and outlined here (8a). Washed cells (~50 mg [wet weight]) were suspended in 500 μl of 6% KOH and incubated at 80°C for 90 min. After cooling to room temperature, 50 μl of glacial acetic acid was added. Insoluble material was washed twice with water and resuspended in 250 μl of 50 mM sodium phosphate (pH 6.3); 2 mg of *Streptomyces griseus* chitinase (Sigma) was added, and tubes were incubated at 25°C with gentle agitation for 2 h. Tubes were centrifuged at 15,000 × *g* for 5 min at room temperature, and 250 μl of supernatant was transferred to a fresh tube to which 1 mg of *Helix pomatia* β-glucuronidase (Sigma) was added. Tubes were incubated at 37°C for 2 h with gentle agitation and then assayed for *N*-acetylglucosamine content.

Measurement of Mpk1p-HA phosphotyrosine content. Mid-log-phase cultures of cells expressing Mpk1p-HA or a vector-only control were exposed to calcofluor white (40 μg/ml for 30 min), α-factor (4 μM for 3 h), or high temperature (37°C for 3 h); 1 ml of culture was centrifuged (15,000 × *g*, 30 s, room temperature), the supernatant was aspirated, and the cell pellet was resuspended in 50 μl of 1× SDS loading buffer and boiled for 4 min. Cell debris was pelleted by centrifugation, and 10 μl of supernatant per sample was subjected to SDS-PAGE and Western blotting. Tyrosine phosphorylation of proteins was visualized by incubation of blots with the phosphotyrosine-specific antibody 4G10 (gift from J. Lee) at 1:3,300 dilution and anti-mouse horseradish peroxidase-conjugated secondary antibody at 1:2,000. Blots were then stripped and reprobed with the anti-HA monoclonal antibody 12CA5 to verify equal loading of Mpk1p-HA in each lane.

RESULTS

***MID2* stimulates Skn7p transcriptional activity.** Skn7p, a transcription factor containing a region of homology to bacterial two-component response-regulator proteins, was isolated by Brown et al. (6) as a high-copy-number suppressor of growth defects in *kre9Δ* mutants. A screen was performed to identify genes which, when overexpressed, would stimulate the Skn7p-LexA-dependent transcription of a $(lexA_{op})_4$-*HIS3* reporter (38). In this procedure, the L40 reporter strain carrying Skn7p-LexA was transformed with a Yep13-based multicopy genomic bank. Plasmid clones were extracted from colonies which could grow on synthetic medium lacking histidine and including 10 mM 3-amino-1,2,4-triazole (3AT) to squelch His3p activity resulting from basal transcription of *HIS3*.

Ten groups of activator of *SKN7* (*ASK*) clones, *ASK1* to *ASK10*, were identified. Sequence analysis revealed that *ASK5*, *ASK7*, and *ASK9* contained a common gene, *YLR332W* (*MID2*). We subcloned the *MID2*, gene including 627 nucleotides 5′ of the codon for the start methionine and 737 nucleotides 3′ of the stop codon, into pRS425 and directly tested the ability of *MID2* to stimulate Skn7p-LexA transcriptional activity. Multicopy *MID2* is able to strongly induce Skn7p-LexA activity compared to a vector-only control, permitting reporter strain growth on medium lacking histidine and containing 30 mM 3AT (Fig. 1). This effect is dependent on an interaction between *MID2* and *LEXA-SKN7* since overexpression of *MID2* alone does not activate transcription of the reporter (not shown). We also measured the induction of β-galactosidase activity from the $(lexA_{op})_8$-*lacZ* locus and found that multicopy *MID2* was able to induce a 7- to 10-fold, Skn7-LexA-dependent increase in β-galactosidase activity (not shown).

Characterization and subcellular localization of Mid2p. *MID2* is predicted to encode a type I membrane-spanning protein containing an N-terminal secretion signal sequence followed by a domain of approximately 200 amino acids consisting of ~62% serine and threonine residues. The C-terminal third of the protein contains a single predicted transmembrane

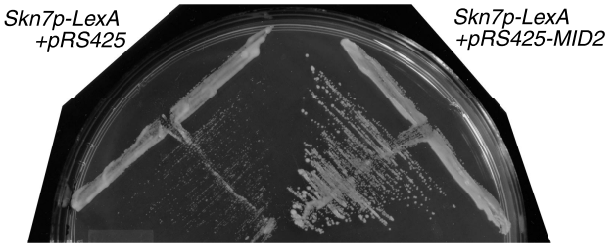

FIG. 1. Multicopy *MID2* activates Skn7p-LexA-dependent transcription of *HIS3*, which allows growth on medium lacking histidine. Reporter strains containing Skn7p-LexA and either pRS425 (TK60) or pRS425-*MID2* (TK61) were grown on selective medium lacking histidine and containing 30 mM 3AT.

domain and a short charged domain rich in aspartic acid residues, suggested to resemble a calcium binding domain (36). Although Mid2p has overall structural similarity to members of the *WSC* family, there are two important differences. Firstly, Mid2p does not contain an extracellular cysteine-rich motif that is characteristic of the Wsc proteins. Second, apart from the repetitive serine/threonine-rich region, there is no statistically significant amino acid residue sequence similarity between Mid2p and Wsc proteins.

To examine physical characteristics of Mid2p, a functional HA-tagged protein (Mid2p-HA) was generated. After proteolytic processing of the signal peptide, Mid2p-HA is predicted to have a molecular mass of approximately 39 kDa. However, Mid2p-HA migrates with an apparent molecular mass of approximately 200 kDa on SDS-PAGE (Fig. 2A, lane b). The predicted type I orientation of Mid2p suggests that if Mid2p were plasma membrane localized, the serine/threonine-rich region would reside on the exterior face of the cell. Since serine/threonine-rich regions of extracellular protein domains can receive O-linked mannosylation as the protein travels through the secretory pathway (45), we examined Mid2p for evidence of this modification. When isolated from *pmt1*Δ *pmt2*Δ mutants (deficient in O-linked mannosylation [30]), Mid2p-HA migrates on SDS-PAGE close to the predicted size of 39 kDa (Fig. 2A, lane d), displaying a shift of roughly 160 kDa compared to Mid2p-HA expressed in wild-type cells. To verify that it was the serine/threonine domain that was the recipient of the O-mannosylation, we excised this region from Mid2p-HA, generating ΔS/T Mid2p-HA. On SDS-PAGE, ΔS/T Mid2p-HA also migrates near its predicted molecular mass of 23 kDa (Fig. 2B), strongly suggesting that the serine/threonine-rich region is the recipient site of O-linked mannosylation. ΔS/T Mid2p-HA localizes to the same subcellular location as Mid2p-HA (not shown; see below); however, pRS316-ΔS/T Mid2p-HA is unable to complement a *mid2*Δ mutant for sensitivity to α-factor, indicating that Mid2p requires the serine-threonine rich domain for activity. Together, these results suggest that extensive, functionally important modification of Mid2p occurs on the extracellular serine/threonine-rich region.

To verify the prediction that Mid2p is an integral membrane protein, partially purified extracts from cells expressing Mid2p-HA were fractionated into supernatant (soluble) and pellet (membrane-containing) portions by centrifugation. Mid2p-HA is found exclusively in the low-speed (15,000 × *g*)-spin pellet fraction, implying membrane association (Fig. 2C). To test whether this membrane association was peripheral or integral, partially purified, membrane-containing cell extracts were treated prior to ultracentrifugation with sodium chloride, sodium carbonate, or urea to disrupt peripheral interactions or with Triton X-100 to disrupt integral membrane association. Only Triton X-100 was capable of solubilizing a significant proportion of Mid2p-HA (Fig. 2C), strongly suggesting that Mid2p-HA is an integral membrane protein. There does not appear to be a fraction of Mid2p-HA covalently associated with the cell wall since treatment of purified cell wall fractions with β-1,3-glucanase (either laminarinase or Quantazyme) before solubilization of proteins by treatment with SDS does not release any detectable Mid2p-HA (not shown).

Direct immunofluorescence microscopy was performed to establish the subcellular localization of Mid2p. A functional Mid2p-GFP fusion protein was constructed by inserting *GFP* immediately upstream of the *MID2* stop codon. Examination of fluorescing cells maintaining either centromeric (not shown) or multicopy (Fig. 2D) Mid2p-GFP reveals Mid2p-GFP distribution to be largely confined to the periphery of cells, consistent with a plasma membrane localization. Expression of native GFP alone produces a diffuse fluorescence pattern

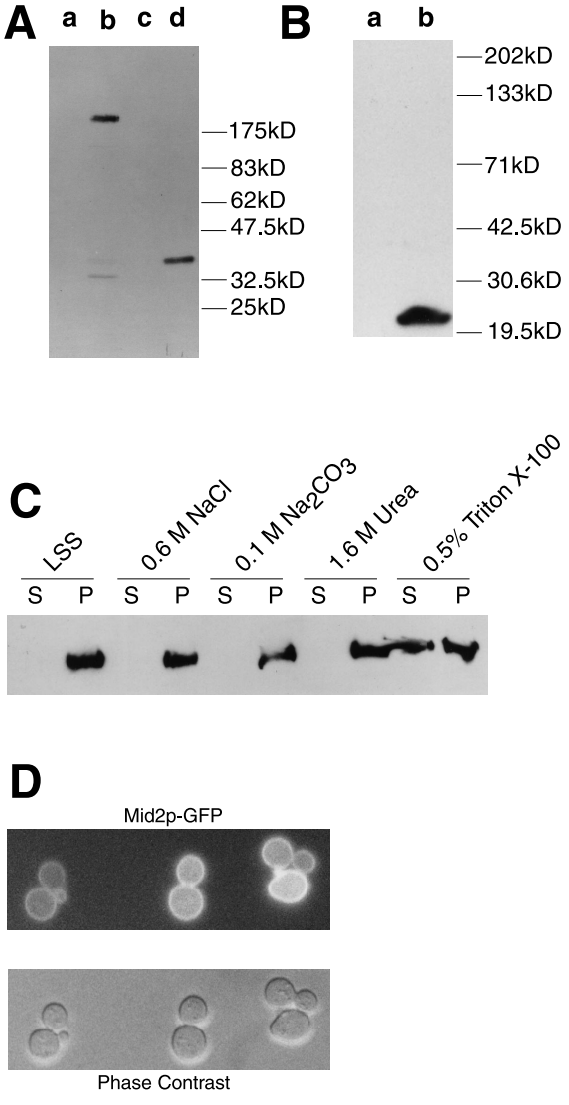

FIG. 2. Cell biology of Mid2p. (A) Immunoblot analysis of cell extracts from TK82 (vector only) (lane a), TK84 (*MID2-HA*) (lane b), *pmt1*Δ *pmt2*Δ (vector only) (lane c), and *pmt1*Δ *pmt2*Δ (*MID2-HA*). (B) Immunoblot analysis of cell extracts from TK82 (vector only) (lane a) and TK85 (ΔS/T-*Mid2p-HA*) (lane b). (C) Immunoblot analysis of cell fractions from TK84 to demonstrate membrane association of Mid2p. LSS, low-speed-spin pellet fraction. (D) In cells expressing pRS426-*MID2-GFP* (TK98), Mid2p-GFP is localized to the cell periphery.

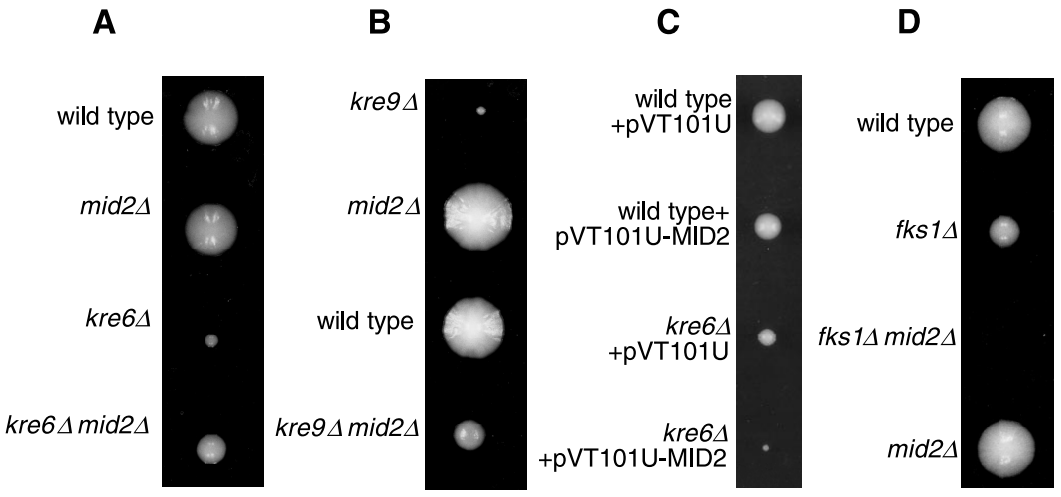

FIG. 3. Deletion of *MID2* has effects on growth of different cell wall mutants. (A) Representative tetratype tetrad from TK101 (*kre6*Δ *mid2*Δ heterozygous diploid). (B) Representative tetratype tetrad from TK102 (*kre9*Δ *mid2*Δ heterozygous diploid). (C) Single cells containing the indicated plasmids were placed on selective agar and grown at 30°C for 4 days. Photo is representative of effect seen in three isolates each of three transformations. (D) Representative tetratype tetrad from TK103 (*fks1*Δ *mid2*Δ heterozygous diploid).

throughout the cell (not shown). Indirect immunofluorescence of cells expressing Mid2p-HA revealed an identical pattern of staining (not shown). No polarized localization of Mid2p-GFP to specific regions of the surface such as the bud tip or bud neck was detected; however, approximately 20% of α-factor-treated cells ($n = 100$) display faint preferential staining at the subapical region of the mating projection (not shown).

Interactions between *MID2* and cell wall biosynthesis genes. Since the O-mannosylated, extracellular domain of Mid2p is predicted to be oriented toward the cell wall, we explored a possible relationship between Mid2p and the cell wall by searching for genetic interactions between *MID2* and genes known to be involved in cell wall construction. Deletion of *MID2* in two viable but slow-growing β-1,6-glucan synthesis mutants, *kre6*Δ (42) and *kre9*Δ (5), partially restores growth rate (Fig. 3A, and B). This effect is not due to differential timing of spore germination since increased growth rate in the absence of *MID2* (~20% reduction in doubling time) is observed for *kre6*Δ cells cultured in liquid medium. Also, reintroduction of *MID2* on a centromeric plasmid causes *kre6*Δ *mid2*Δ cells and *kre9*Δ *mid2*Δ cells to resume slower growth (not shown). Interestingly, high-copy-number expression of *MID2* in the *kre6*Δ mutant has a strong negative effect on growth rate (Fig. 3C). Optical density measurement of cell growth in liquid culture revealed that high-copy-number expression of *MID2*(pRS426-*MID2*) in *kre6*Δ cells resulted in a ~300% increase in doubling time compared to a vector-only control. This reduction in growth rate is much more pronounced in *kre6*Δ mutants than in wild-type cells, where doubling time increases by only 15% over a vector-only control for cells carrying pRS426-*MID2*. Interestingly, high-copy-number expression of *MID2* in the growth-deficient *pmt1*Δ *pmt2*Δ mutants, where Mid2p is undermannosylated, also results in a reduction in growth rate. This finding suggests that although the serine/threonine-rich domain itself is indispensable for Mid2p activity, extensive O-linked mannosylation of this region may not be totally essential for Mid2p function.

Examination of cell wall glucan content revealed that wild-type and *mid2*Δ cells have no differences in β-1,6- and β-1,3-glucan content. Similarly, *kre6*Δ and *kre6*Δ *mid2*Δ mutants have comparable levels of both glucan species (not shown), suggesting that at least for the *kre6*Δ mutant, increased growth rate induced by loss of *MID2* is not caused by a restoration of β-1,6-glucan synthesis. To determine if *MID2* genetically interacts with the β-1,3-glucan synthesis pathway, we examined the consequence of loss of *MID2* in *fks1*Δ mutants (13, 17, 40). In contrast to the restorative effect that deletion of *MID2* had in β-1,6-glucan mutants, loss of *MID2* in *fks1*Δ cells causes inviability (Fig. 3D). This phenotype is not reversible by the addition of 1 M sorbitol or 30 mM calcium chloride (not shown). Overexpression of *MID2* in an *fks1*Δ mutant does not result in an inhibition of growth like that seen in *kre6*Δ mutants with high-copy-number *MID2* (not shown).

***MID2* affects chitin synthesis under stress conditions.** Although chitin comprises a small percentage of the cell wall weight, its contribution to wall integrity is vital. Calcofluor white is a fluorescent dye that intercalates into nascent chitin chains, preventing microfibril assembly (15). At sufficient concentrations, calcofluor white can kill cells through interference with cell wall assembly. *mid2*Δ cells display significant resistance to calcofluor white. At a calcofluor white concentration of 20 μg/ml on rich medium, wild-type cells are killed whereas *mid2*Δ cells can grow without apparent inhibition (Fig. 4A).

Since resistance to calcofluor white is a phenotype often associated with defects in chitin synthesis, one possibility is that calcofluor white resistance of *mid2*Δ cells is a consequence of reduced chitin synthesis. Measurement of chitin levels in wild-type and *mid2*Δ cells revealed that they have identical chitin contents when grown in rich (YEPD) medium, suggesting that Mid2p is not required for basal chitin production under such optimum growth conditions (Table 3, condition A). Because exposure to calcofluor white increases chitin production in vivo (43), we tested whether *MID2* is required for synthesis of supplemental chitin by measuring the chitin content of cells that had been challenged with sublethal concentrations of calcofluor white. We then calculated the amount of new chitin synthesized in response to calcofluor white challenge by subtracting the amount of chitin produced under nonstressed conditions from the total chitin measured after calcofluor white exposure. Interestingly, *mid2*Δ mutants contained 40% less new, stress-induced, total cell wall chitin than wild-type cells when cultures were grown in the presence of 10 μg of calcofluor white per ml for 2 h prior to harvesting (Table 3, condition B). This attenuation of calcofluor white-induced

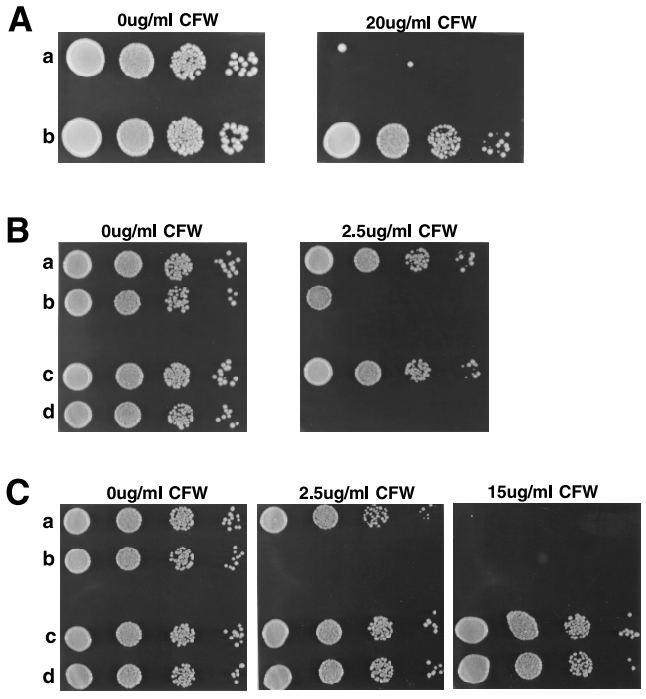

FIG. 4. Dosage of *MID2* affects sensitivity to calcofluor white. Mid-log-phase cells were diluted to a concentration of 3×10^6 cells/ml; 5 μl of this suspension and three subsequent 10-fold serial dilutions were each spotted onto the indicated medium. (A) SEY6210**a** (wild type) (row a) and TK88 (*mid2*Δ) (row b) cells were spotted onto YEPD containing 0 and 20 μg of calcofluor white (CFW) per ml. (B) TK82 [wild type (pRS426)] (row a), TK83 [wild type (pRS426-*MID2*)] (row b), TK86 [wild type (pVT101U)] (row c), and TK87 [wild type (pVT101U-*MID2*)] (row d) were spotted on uracil dropout medium containing 0 and 2.5 μg of calcofluor white per ml. (C) TK86 (row a), TK87 (row b), TK99 [*chs3*Δ (pVT101U)] (row c), and TK100 [*chs3*Δ (pVT101U-*MID2*)] (row d) were spotted onto uracil dropout medium containing 0, 2.5, and 15 μg of calcofluor white per ml.

chitin synthesis is likely to be at least part of the cause of calcofluor white resistance in *mid2*Δ cells.

To determine if Mid2p is required for supplementary chitin synthesis under a broader range of cell wall stresses, we looked for Mid2p-dependent changes in cellular chitin content in two other circumstances. It has been observed that cell wall mutants typically have higher cell wall chitin levels than wild-type cells (39, 41). Analysis of chitin content revealed that *kre6*Δ cells have >2.5-fold more total chitin than wild-type cells. Similar to the effect seen in calcofluor white-challenged cells, loss of *MID2* causes a small but significant decrease (~28%) in extent of stress-induced chitin synthesis in *kre6*Δ mutants (Table 3, condition C). Another situation known to increase chitin production is shmoo formation in response to mating pheromone (44). After induction of projection formation by α-factor, *MAT***a** *mid2*Δ mutants had synthesized almost 80% less new chitin than wild-type cells (Table 3, condition D). These observations suggest that Mid2p is partially required for production of supplementary wall chitin under conditions of wall damage (by mutation or calcofluor white) or morphological change (shmoo formation).

To further address the relationship between *MID2* and chitin synthesis, growth of cells overexpressing *MID2* was examined on calcofluor white-containing medium. Cells harboring *MID2* on a 2 μm plasmid have reduced viability at a calcofluor white concentration of 2.5 μg/ml, and cells expressing *MID2* from the strong constitutive *ADH1* promoter at 2 μm levels are completely inviable on calcofluor white at 2.5 μg/ml (Fig. 4B). Since calcofluor white resistance in *mid2*Δ cells is associated with reduced supplementary chitin synthesis, this finding suggests that overexpression of *MID2* may cause an increase in wall chitin content, conferring hypersensitivity to this drug. Indeed, analysis of total chitin revealed that cells carrying *ADH1* promoter-driven *MID2* had approximately 250% more chitin than cells without multicopy *MID2* (Table 1, condition E).

Because Chs3p is responsible for the bulk of lateral wall and bud scar chitin, and deletion of *CHS3* leads to a 10-fold reduction in total cellular chitin content and strong resistance to calcofluor white, we next tested whether the hypersensitivity to calcofluor white caused by *MID2* overexpression is mediated through Chs3p activity. Spot testing of *chs3*Δ cells containing multicopy *MID2*, with either its own or the *ADH1* promoter, on calcofluor white-containing medium revealed that *CHS3* is required for high-copy-number *MID2* to confer calcofluor white hypersensitivity (Fig. 4C). This finding suggests that Mid2p may ultimately affect extra chitin synthesis through some form of regulation of Chs3p activity.

***MID2* interacts with the cell integrity pathway.** To identify additional *MID2* interactors, we performed a screen for multicopy suppressors of the *mid2*Δ *fks1*Δ synthetic lethality [plasmids were selected for the ability to promote growth in *mid2*Δ *fks1*Δ (pRS316-*FKS1*) cells after loss of pRS316-*FKS1* was promoted by replication onto medium containing 5-fluoroorotic acid]. Two of the genes identified as *mid2*Δ *fks1*Δ suppressors were *PKC1* and *WSC1*. Several genetic interactions between *MID2* and *WSC1* suggest that these genes possess overlapping activities. First, *mid2*Δ *wsc1*Δ cells are inviable at 22 or 30°C on YEPD medium. Inclusion of sorbitol (between 0.3 and 1 M) in medium permits partial restoration of growth,

TABLE 3. Measurement of total cellular chitin

Condition	Strain	nmoles of GlcNAc/mg (wt) of cells (mean ± SD)	Increase from control (nmol of GlcNAc/mg [wet wt] of cells)	*MID2*-dependent change (%)
A (YEPD [control])	Wild type	3.54 ± 0.06		
	*mid2*Δ	3.60 ± 0.31		
B (YEPD + calcofluor white [10 μg/ml], 2 h)	Wild type	8.96 ± 0.16	5.42	
	*mid2*Δ	6.82 ± 0.14	3.22	−40
C (YEPD)	*kre6*Δ	9.50 ± 0.43	5.96 (from wild type)	
	*kre6*Δ *mid2*Δ	7.90 ± 0.08	4.30 (from *mid2*Δ)	−28
D (YEPD + 4 μM α-factor, 3 h)	Wild type	5.05 ± 0.19	1.51	
	*mid2*Δ	3.91 ± 0.05	0.31	−79
E (YNB [uracil dropout])	Wild type carrying pVT101U	4.65 ± 0.65		
	Wild type carrying pVT101U-*MID2*	11.87 ± 0.22		+255

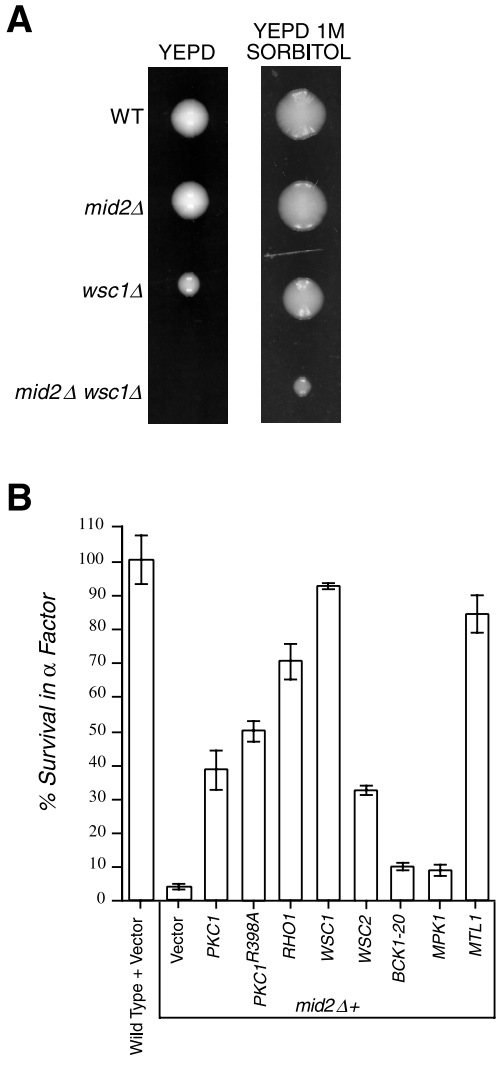

FIG. 5. Genetic interactions between *MID2* and members of the cell integrity pathway. (A) Representative tetratype tetrads of TK104 (*mid2*Δ *wsc1*Δ heterozygous diploid) dissected onto either YEPD or YEPD plus 1 M sorbitol. YEPD plates were incubated for 60 h at 30°C, YEPD–1 M sorbitol plates were incubated for 80 h at 30°C. WT, wild type. (B) Members of the cell integrity pathway suppress α-factor-induced death in *mid2*Δ mutants. Wild-type cells containing pRS426 vector only and *mid2*Δ mutants carrying pRS426, YEP13-*PKC1*, pBM743-*PKC1*^{R398A} (GAL-driven, hyperactive *PKC1*), pRS426-*RHO1*, pRS426-*WSC1*, pRS426-*WSC2*, pRS316-*BCK1-20* (hyperactive *BCK1*), YEP352-*MPK1*, and pRS425-*MTL1* in liquid medium were exposed to α-factor. Percentage of survival was measured by spreading liquid medium before and after α-factor exposure (330 mn) on petri dishes and counting colonies derived from single cells.

suggesting that *mid2*Δ *wsc1*Δ mutants, like *pkc1*Δ mutants, are prone to lysis without osmotic support (Fig. 5A). When transferred from osmotically supported medium to YEPD, *mid2*Δ *wsc1*Δ mutants arrest growth with a small bud. After 36 h on YEPD, approximately 85% of *mid2*Δ *wsc1*Δ cells have small buds, while between 6 and 8% of wild-type, *mid2*Δ and *wsc1*Δ cells display a small bud (more than 150 cells counted per genotype). Further suggesting a functional relationship between *MID2* and *WSC1*, high-copy-number expression of *MID2* partially suppresses the growth defect of *wsc1*Δ mutants (not shown). Finally, overexpression of *WSC1* is able to relieve the sensitivity of *mid2*Δ cells to α-factor (Fig. 5B). Together, these findings indicate a functional overlap between Mid2p and Wsc1p.

Since Wsc1p and its homologs have been implicated in Pkc1p activation, and the *mid2*Δ *wsc1*Δ small-budded terminal phenotype resembles that of cells lacking Pkc1p activity (28), we examined the possibility that Mid2p can also contribute to regulation of the *PKC1-MPK1* pathway. Like *pkc1*Δ mutants, *mid2*Δ *pkc1*Δ cells are inviable on medium without osmotic support; however, these double mutants are able to grow at a rate similar to that of *pkc1*Δ mutants on medium containing 1 M sorbitol at both 22 and 30°C (not shown). Moreover, multicopy *MID2* does not alter the growth rate of *pkc1*Δ cells (not shown), suggesting that genetically, *PKC1* acts downstream of *MID2*.

To further explore the potential role of Mid2p in *PKC1-MPK1* pathway regulation, we examined whether Mid2p influences Mpk1p activation. The Mpk1p MAP kinase is activated through tyrosine phosphorylation during mating projection formation (8, 49). We found that compared to wild-type cells, *mid2*Δ mutants have substantially less tyrosine phosphorylation on Mpk1p-HA after exposure of cells to α-factor (Fig. 6A). This observation suggests that underactivation of the cell integrity pathway might be, at least in part, responsible for pheromone-induced death in *mid2*Δ mutants. The finding that overexpression of *PKC1*, *PKC1*^{R398A} (a hyperactive allele), *RHO1*, *WSC1*, and *WSC2* can suppress α-factor-induced death in *mid2*Δ mutants (Fig. 5B) independently supports this conclusion. However, expression of either *bck1-20* (a hyperactive allele of *BCK1*), or *MPK1* does not suppress this phenotype, and at high concentrations of pheromone (>4 μM) only some of the most upstream elements of the cell integrity pathway, including *RHO1*, *WSC1*, and *WSC2*, can prevent mating pheromone-induced death (not shown).

To explore the genetic relationship between *MID2* and *RHO1*, we tested whether *MID2* overexpression suppresses *rho1*Δ mutants. Because cells lacking Rho1p are inviable, even at low temperature on medium with osmotic support, *rho1*Δ heterozygous diploids were transformed with high-copy-number *MID2* and then sporulated, and the resulting asci were dissected. No viable *rho1*Δ mutants were recovered from 36 tetrads analyzed, suggesting that high-copy-number *MID2* is unable to suppress the lack of Rho1p. Since overexpression of *RHO1* can suppress α-factor-induced death in *mid2*Δ mutants but high-copy-number *MID2* cannot suppress inviability of *rho1*Δ mutants, it appears that Mid2p may act upstream of, or in parallel with, Rho1p.

Interestingly, Mpk1p-HA tyrosine phosphorylation is also increased in wild-type cells in response to exposure to calcofluor white. This effect is dependent on the presence of Mid2p, since there is a deficit of this phosphorylation on Mpk1-HA in *mid2*Δ cells (Fig. 6B). *MID2*-dependent increase in tyrosine phosphorylation of native Mpk1p in response to calcofluor white and mating pheromone is not readily apparent in Fig. 6A and B, perhaps due to lower relative abundance of native Mpk1p versus (2 μm-borne) Mpk1-HA. Also, for the chosen time points, a lower extent of tyrosine phosphorylation on Mpk1-HA is seen for calcofluor white and mating factor exposure than is observed for high-temperature growth (Fig. 6C), suggesting that differences in phosphorylation state for native Mpk1p in these panels may be below the detection threshold. In other assay conditions, we observe clear *MID2* dependence for native Mpk1p tyrosine phosphorylation in response to calcofluor white and mating factor (not shown). Deletion of *MPK1* results in calcofluor white hypersensitivity, likely due to gross disturbances in cell wall construction. Saliently, overexpression of *MPK1*, like overexpression of *MID2*, also results in a *CHS3*-dependent hypersensitivity to calcofluor white (not shown). This effect is *MID2*-dependent since overexpression of

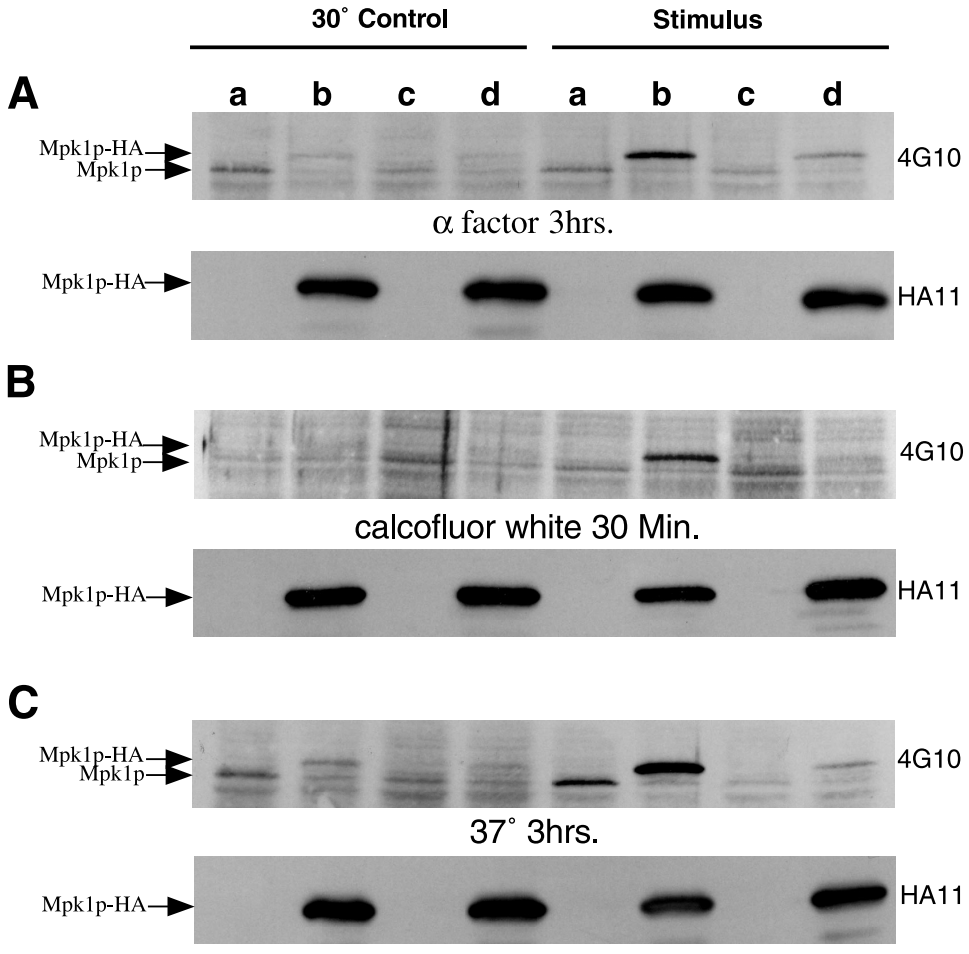

FIG. 6. Immunoblot analysis of Mpk1p-HA tyrosine phosphorylation. Lanes are loaded with equal amounts of extracts from strains TK96 [wild type (pFL44)] (lanes a), TK97 [wild type (pFL44-*MPK1-HA*)] (lanes b), TK93 [*mid2*Δ (pFL44)] (lanes c), and TK94 [*mid2*Δ(pFL44-*MPK1-HA*)] (lanes d). Cultures exposed to α-factor (A), calcofluor white (B), or high-temperature growth (C) were harvested at the indicated times, and total cell proteins were subject to SDS-PAGE and Western blotting. In the top panel of each pair, tyrosine phosphorylation of Mpk1p-HA is detected by antiphosphotyrosine antibody 4G10. In the second panel of each pair, equal loading of Mpk1p-HA is demonstrated by anti-HA antibody HA11.

MPK1 does not bypass the resistance to calcofluor white displayed by *mid2*Δ cells (not shown).

Finally, we examined whether induction of tyrosine phosphorylation of Mpk1p-HA during periods of high-temperature stress requires *MID2*. Although *mid2*Δ cells do not have a growth defect at 37°C, induction of tyrosine phosphorylation of Mpk1p-HA was significantly impaired in *mid2*Δ mutants compared to wild-type cells (Fig. 6C). Together, these observations suggest a role for Mid2p in activation of the Mpk1p MAP kinase cascade under a variety of stress conditions.

Identification of a Mid2p functional homolog. The *S. cerevisiae* genome contains a gene, *YGR023W*, which encodes a 551-amino-acid residue protein with both structural and amino acid sequence similarity to Mid2p [W. U. Blast V2.0 P(N) value of $1.2e^{-27}$]. We will refer to *YGR023W* as *MTL1* (*MID2*-like 1). To initiate the characterization of *MTL1*, we disrupted its entire ORF. Unlike *mid2*Δ cells, *mtl1*Δ mutants in the SEY6210 strain background have no distinguishable phenotype when challenged with temperature extremes, oxidative and osmotic stresses, α-factor, calcofluor white, or mutation of the *KRE6* or *FKS1* cell wall synthesis gene (not shown). While *mtl1*Δ single mutants are not hypersensitive to caffeine, *mid2*Δ cells are mildly more susceptible than wild-type cells, and *mid2*Δ *mtl1*Δ double mutants show strong sensitivity to this drug. This phenotype appears to be the result of cell lysis since it is suppressible by the inclusion of 1 M sorbitol in the growth medium (not shown). Caffeine sensitivity of the *mid2*Δ *mtl1*Δ mutant is also suppressible by overexpression of *WSC2*; however, multicopy *WSC1*, *RHO1*, *PKC1*, *BCK1*, and *MPK1* do not bypass this phenotype. Finally, although *mid2*Δ *mtl1*Δ double mutants are no more sensitive to α-factor than *mid2*Δ cells (not shown), high-copy-number expression of *MTL1* from either its own promoter or the *ADH1* promoter is able to suppress the caffeine (not shown) and α-factor sensitivity of *mid2*Δ cells (Fig. 5B), suggesting that *MTL1* is a functional gene and that the activity of Mtl1p may be related to or overlap the activity of Mid2p.

DISCUSSION

Mid2p is an O-mannosylated, plasma membrane protein. In this work, we offer evidence that Mid2p may potentially sense cell wall state and act to initiate a cellular response involving both chitin synthesis and the *PKC1-MPK1* cell integrity pathway. Mid2p is a type I integral membrane protein which localizes to the plasma membrane and contains a large, extensive-

ly O-mannosylated extracellular serine/threonine-rich region. Removal of the serine/threonine-rich region does not affect the targeting of Mid2p; however, ΔS/T Mid2p is unable to complement *mid2*Δ cells, suggesting that this domain is required for Mid2p activity. This observation contrasts with the findings for Gas1p and Kre1p, two glycosyl phosphatidylinositol-anchored proteins involved in cell wall synthesis, where deletion of the serine/threonine-rich sequences does not greatly affect function of these proteins (4, 18). O-linked mannosylation could cause the extracellular region to adopt a stiff and extended conformation (23) that reaches from the plasma membrane toward the cell wall, perhaps interacting with it. In Mid2p, this region is unlikely to play a direct enzymatic role since it is largely composed of repetitive noncomplex amino acid sequence, and it lacks any similarity to known enzymatic motifs. An intriguing possibility is that the extracellular domain can act as a sensor of cell wall state.

***MID2* interacts with genes required for cell wall construction and cell wall integrity signaling.** We isolated *MID2* as an activator of the Skn7p transcription factor. Skn7p appears to affect a number of cellular processes, including cell wall biosynthesis. *SKN7* was identified by Brown et al. (6) as a high-copy-number suppressor of the *kre9*Δ mutant, and it was later demonstrated that Skn7p may function in parallel with Pkc1p since overexpression of *SKN7* can suppress the lysis defect of *pkc1*Δ mutants, and *skn7*Δ *pkc1*Δ cells are inviable, even on medium containing osmotic support (7). Recently, Alberts et al. (1) have shown that Rho1p and Skn7p physically interact and that the domain in Skn7p that mediates this interaction is important for activity. It is not clear how Mid2p might stimulate Skn7p transcriptional activity. Since *RHO1* appears to have interactions with both *SKN7* and *MID2*, one avenue of future research will be to examine whether Rho1p mediates a Mid2p-Skn7 interaction.

Deletion of *MID2* causes significant changes in growth rate or viability for a variety of cell wall synthesis mutants. It is curious that for the β-1,6-glucan mutants examined, loss of *MID2* increases growth rate, while for the β-1,3-glucan mutant *fks1*Δ, deletion of *MID2* causes inviability. One possibility is that reduction of supplementary chitin levels caused by absence of Mid2p is a contributing factor. *fks1*Δ mutants seem to depend heavily on enhanced chitin synthesis to maintain viability since they are supersensitive to nikkomycin Z, a chitin synthase inhibitor (16). Conversely, there is some evidence that attenuation of the chitin synthesis stress response may actually be beneficial in cells lacking proper β-1,6-glucan synthesis, specifically in *kre9*Δ mutants (33). Consistent with this hypothesis, overexpression of *MID2*, which causes hyperaccumulation of chitin, is deleterious to β-1,6-glucan mutants but has little effect on the β-1,3-glucan-deficient mutant *fks1*Δ.

Screens to identify genes which interact with *MID2* uncovered a relationship between *MID2* and several components of a pathway known to promote cell integrity and polarized growth. Caffeine sensitivity of the *mid2*Δ and *mid2*Δ *mtl1*Δ mutants is suppressed by overexpression of *WSC2*, high-copy-number *WSC1* and *PKC1* suppress *mid2*Δ *fks1*Δ synthetic lethality, and multicopy *PKC1*, *RHO1*, *WSC1*, and *WSC2* suppress lethality in *mid2*Δ *MAT***a** cells exposed to α-factor. Additionally, *mid2*Δ *wsc1*Δ mutants are inviable without osmotic support and exhibit defects similar to those observed in *pkc1*Δ mutants. Finally, we find that during shmoo formation, high-temperature growth, or exposure to calcofluor white, tyrosine phosphorylation of Mpk1p, a downstream target of Pkc1p, is reduced in *mid2*Δ cells. Interestingly, although *mid2*Δ mutants have reduced tyrosine phosphorylation of Mpk1p in response to high-temperature growth, these cells are not deficient for growth at high temperature. It is possible that there is sufficient remaining Mpk1p activity to allow cells to survive high-temperature stress or that some other mechanism is able to compensate for underactivation of this pathway. Strain differences may also play some role here, since we do not observe high-temperature sensitivity in *wsc1*Δ mutants as reported by Verna et al. (47).

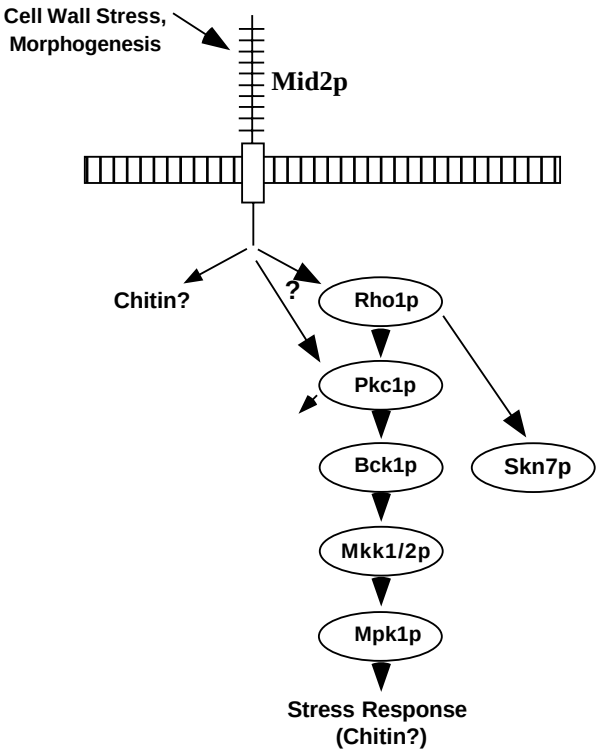

FIG. 7. Model of Mid2p activity. Mid2p responds to cell wall stress by activating the cell integrity pathway and increasing chitin synthesis.

Although *mid2*Δ cells have no apparent vegetative growth defects, shmoo formation, mutation of cell wall synthesis genes, and exposure to calcofluor white cause *mid2*Δ mutants to manifest phenotypes. One possibility is that Mid2p and perhaps members of the *WSC* family act indirectly, through effects on cell wall structure, to activate the *PKC1-MPK1* pathway. In an alternative model, Mid2p might sense cell wall stress and directly act to increase activity in the cell integrity pathway to counteract damage (Fig. 7). Under nonstressed conditions, Mid2p activity might be low, or not be required, and Wsc1p and its homologs may be largely responsible for Pkc1p activation. However, under circumstances of cell wall stress, in the absence of Mid2p, the cell integrity machinery would be unresponsive and would continue to function at a level more appropriate for low or nonstress situations.

This model explains why some of the phenotypes observed in *mid2*Δ mutants contrast with those displayed by other mutants in the cell integrity pathway. For example, strains carrying mutations such as *wsc1*/*2*/*3*Δ, *pkc1*Δ, *bck1*Δ, or *mpk1*Δ are prone to cell lysis in the absence of osmotic support. These genes are required for normal function of the cell integrity pathway under all growth conditions. In their absence, construction and maintenance of the cell wall is defective, making the wall highly susceptible to damage. *mid2*Δ mutants have apparently normal cell walls when grown in ordinary conditions. However, in stress situations, such as exposure to calcofluor white or α-factor, *mid2*Δ mutants have an attenuated

response compared to wild-type cells, as indicated by the reduced amount of new chitin synthesized and by the reduced extent of tyrosine phosphorylation on Mpk1p.

Preliminary investigation of *MTL1*, the only *S. cerevisiae* gene encoding a protein with significant sequence similarity to Mid2p, revealed that it may have a function in common with *MID2*. Although *mtl1*Δ mutants do not display many of the phenotypes that *mid2*Δ cells do, sensitivity to caffeine is much greater in *mid2*Δ *mtl1*Δ double mutants than in either single mutant. Additionally, multicopy *MTL1* can suppress α-factor sensitivity of *mid2*Δ cells. Further research may reveal whether Mtl1p is required for responding to different stresses than Mid2p, signals to a different pathway than Mid2p, or is important under physiological conditions different from those used in this study.

The effect of Mid2p on chitin synthesis depends ultimately on Chs3p, since overexpression of *MID2* in *chs3*Δ mutants cannot confer hypersensitivity to calcofluor white. We suggest two ways in which Mid2p might affect chitin synthesis. Mid2p might directly interact with the chitin synthase complex, increasing its activity during stress periods. Alternatively, the activity of Chs3p might be regulated by a downstream target of Mid2p, such as Mpk1p.

Cells face a demanding variety of stresses in their natural environments and must respond accordingly. Our results provide new insights into the processes by which yeast cells sense and respond to threats against their physical integrity. Mid2p has been identified as a putative sensor of cell wall state that is required for stimulation of activity in the *PKC1-MPK1* MAP kinase pathway under conditions of cell wall stress. Currently, the physiological roles of most serine/threonine-rich membrane proteins are poorly defined. An interesting possibility is that as a class, these proteins act as sensors for a range of environmental stresses and mediate a variety of cellular processes.

ACKNOWLEDGMENTS

We thank S. Nagahashi, M. Rajavel, T. Roemer, and P. A. Delley for helpful and stimulating discussion; R. C. Stewart and J. L. Brown for designing and performing the original *ASK* screen; S. Véronneau and T. Nguyen for sequencing; and S. Shahinian for critical input on the manuscript. We also thank C. Bulawa for assistance with the chitin assay protocol and for providing the *chs3*Δ*::LEU2* plasmid, M. Snyder for providing multicopy *MPK1-HA*, *BCK1*, *MKK1*, and *PKC1*, and M. Rajavel for providing pRS316-*BCK1-20*, and pBM743-*PKC1*^{R398A}.

This work was supported by an NSERC operating grant.

REFERENCES

1. **Alberts, A. S., N. Bouquin, L. H. Johnston, and R. Treisman.** 1998. Analysis of RhoA-binding proteins reveals an interaction domain conserved in heterotrimeric G protein beta subunits and the yeast response regulator protein Skn7. J. Biol. Chem. **273:**8616–8622.
2. **Banuett, F.** 1998. Signalling in the yeasts: an informational cascade with links to the filamentous fungi. Microbiol. Mol. Biol. Rev. **62:**249–274.
3. **Bickle, M., P. A. Delley, A. Schidt, and M. N. Hall.** 1998. Cell wall integrity modulates RHO1 activity via the exchange factor ROM2. EMBO J. **17:**2235–2245.
4. **Boone, C., A. Sdicu, M. Laroche, and H. Bussey.** 1991. Isolation from *Candida albicans* of a functional homolog of the *Saccharomyces cerevisiae KRE1* gene, which is involved in cell wall beta-glucan synthesis. J. Bacteriol. **173:**6859–6864.
5. **Brown, J. L., and H. Bussey.** 1993. The yeast *KRE9* gene encodes an O-glycoprotein involved in cell surface β-glucan assembly. Mol. Cell. Biol. **13:**6346–6356.
6. **Brown, J. L., S. North, and H. Bussey.** 1993. *SKN7*, a yeast multicopy suppressor of a mutation affecting β-glucan assembly, encodes a product with domains homologous to prokaryotic two-component regulators and to heat shock transcription factors. J. Bacteriol. **175:**6908–6915.
7. **Brown, J. L., H. Bussey, and R. C. Stewart.** 1994. Yeast Skn7p functions in a eukaryotic two-component regulatory pathway. EMBO J. **13:**5186–5194.
8. **Buehrer, B. M., and B. Errede.** 1997. Coordination of the mating and cell integrity mitogen-activated protein kinase pathways in *Saccharomyces cerevisiae*. Mol. Cell. Biol. **17:**6517–6525.

8a. **Bulawa, C.** Personal communication.

9. **Bulawa, C. E., M. Slater, E. Cabib, J. Au-Young, A. Sburlati, W. L. Adair, and P. Robbins.** 1986. The *S. cerevisiae* structural gene for chitin synthase is not required for chitin synthesis *in vivo*. Cell **46:**213–225.
10. **Cabib, E., T. Drgon, J. Dronova, R. A. Ford, and R. Kollar.** 1997. The yeast cell wall, a dynamic structure engaged in growth and morphogenesis. Biochem. Soc. Trans. **25:**200–204.
11. **Costigan, C., S. Gehrung, and M. Snyder.** 1992. A synthetic lethal screen identifies *SLK1*, a novel protein kinase homolog implicated in yeast cell morphogenesis and cell growth. Mol. Cell. Biol. **12:**1162–1178.
12. **Daniel, J.** 1993. Potentially rapid walking in cellular regulatory networks using the gene-gene interference method in yeast. Mol. Gen. Genet. **240:**245–257.
13. **Douglas, C. M., F. Foor, J. A. Marrinan, N. Morin, J. B. Nielson, A. M. Dahl, P. Mazur, W. Baginsky, W. Li, M. el-Sherbeini, et al.** 1994. The *Saccharomyces cerevisiae FKS1* (*ETG1*) gene encodes an integral membrane protein which is a subunit of 1,3-beta-D-glucan synthase. Proc. Natl. Acad. Sci. USA **91:**12907–12911.
14. **Drgonova, J., T. Drgon, K. Tanaka, R. Kollar, G. C. Chen, R. A. Ford, C. S. Chan, Y. Takai, and E. Cabib.** 1996. Rho1p, a yeast protein at the interface between cell polarization and morphogenesis. Science **272:**277–279.
15. **Elorza, M. V., H. Rico, and R. Sentandreu.** 1983. Calcofluor white alters the assembly of chitin fibrils in *Saccharomyces cerevisiae* and *Candida albicans* cells. J. Gen. Microbiol. **129:**1577–1582.
16. **el-Sherbeini, M., and J. A. Clemas.** 1995. Nikkomycin Z supersensitivity of an echinocandin-resistant mutant of *Saccharomyces cerevisiae*. Antimicrob. Agents Chemother. **39:**200–207.
17. **Eng, W. K., L. Faucette, M. M. McLaughlin, R. Cafferkey, Y. Koltin, R. A. Morris, P. R. Young, R. K. Johnson, and G. P. Livi.** 1994. The yeast *FKS1* gene encodes a novel membrane protein, mutations in which confer FK506 and cyclosporin A hypersensitivity and calcineurin-dependent growth. Gene **151:**61–71.
18. **Gatti, E., L. Popolo, M. Vai, N. Rota, and L. Alberghina.** 1994. O-linked oligosaccharides in yeast glycosyl phosphatidylinositol-anchored protein gp115 are clustered in a serine rich region not essential for its function. J. Biol. Chem. **269:**19695–19700.
19. **Gray, J. V., J. P. Ogas, Y. Kamada, M. Stone, D. E. Levin, and I. Herskowitz.** 1997. A role for the Pkc1 MAP kinase pathway of *Saccharomyces cerevisiae* in bud emergence and identification of a putative upstream regulator. EMBO J. **16:**4924–4937.
20. **Igual, J. C., A. L. Johnson, and L. H. Johnston.** 1996. Coordinated regulation of gene expression by the cell cycle transcription factor SWI4 and the protein kinase C MAP kinase pathway for yeast cell integrity. EMBO J. **15:**5001–5013.
21. **Irie, K., M. Takase, K. S. Lee, D. E. Levin, H. Araki, K. Matsumoto, and Y. Oshima.** 1993. *MKK1* and *MKK2*, which encode *Saccharomyces cerevisiae* mitogen-activated protein kinase-kinase homologs, function in the pathway mediated by protein kinase C. Mol. Cell. Biol. **13:**3076–3083.
22. **Jacoby, J. J., S. M. Nilius, and J. J. Heinisch.** 1998. A screen for upstream components of the yeast protein kinase C signal transduction pathway identifies the product of the *SLG1* gene. Mol. Gen. Genet. **258:**148–155.
23. **Jentoft, N.** 1990. Why are proteins *O*-glycosylated? Trends Biochem. Sci. **15:**291–294.
24. **Kamada, Y., H. Qadota, C. P. Python, Y. Anraku, Y. Ohya, and D. E. Levin.** 1996. Activation of yeast protein kinase C by Rho1 GTPase. J. Biol. Chem. **271:**9193–9196.
25. **Kunkel, T. A., J. D. Roberts, and R. A. Zakour.** 1987. Rapid and efficient site specific mutagenesis without phenotypic selection. Methods Enzymol. **154:**367–382.
26. **Lee, K. S., and D. E. Levin.** 1992. Dominant mutations in a gene encoding a putative protein kinase (BCK1) bypass the requirement for a *Saccharomyces cerevisiae* protein kinase C homolog. Mol. Cell. Biol. **12:**172–182.
27. **Lee, K. S., K. Irie, Y. Gotoh, Y. Watanabe, H. Araki, E. Nishida, K. Matsumoto, and D. E. Levin.** 1993. A yeast mitogen-activated protein kinase homolog (Mpk1p) mediates signalling by protein kinase C. Mol. Cell. Biol. **13:**3067–3075.
28. **Levin, D. E., and E. Bartlett-Heubusch.** 1992. Mutants in the *S. cerevisiae* PKC1 gene display a cell cycle-specific osmotic stability defect. J. Cell Biol. **116:**1221–1229.
29. **Levin, D. E., B. Bowers, C. Y. Chen, Y. Kamada, and M. Watanabe.** 1994. Dissecting the protein kinase C/MAP kinase signaling pathway of *Saccharomyces cerevisiae*. Cell. Mol. Biol. Res. **40:**229–239.
30. **Lussier, M., M. Gentzsch, A. M. Sdicu, H. Bussey, and W. Tanner.** 1995. Protein O-glycosylation in yeast. The PMT2 gene specifies a second protein O-mannosyltransferase that functions in addition to the PMT1-encoded activity. J. Biol. Chem. **270:**2770–2775.
31. **Manning, B. D., R. Padmanabha, and M. Snyder.** 1997. The Rho-GEF Rom2p localizes to sites of polarized cell growth and participates in cytoskeletal functions in *Saccharomyces cerevisiae*. Mol. Biol. Cell **8:**1829–1844.
32. **Marcoux, N., Y. Bourbonnais, P. Charest, and D. Pallota.** 1998. Overexpres-

sion of *MID2* suppresses the profilin deficient phenotype of yeast cells. Mol. Microbiol. **29:**515–526.
33. **Nagahashi, S., M. Lussier, and H. Bussey.** 1998. Isolation of *Candida glabrata* homologs of the *Saccharomyces cerevisiae KRE9* and *KNH1* genes and their involvement in cell wall β-1,6-glucan synthesis. J. Bacteriol. **180:**5020–5029.
34. **Niedenthal, R. K., L. Riles, M. Johnston, and J. H. Hegemann.** 1996. Green fluorescent protein as a marker for gene expression and subcellular localization in budding yeast. Yeast **12:**773–786.
35. **Nonaka, H., K. Tanaka, H. Hirano, T. Fujiwara, H. Kohno, M. Umikawa, A. Mino, and Y. Takai.** 1995. A downstream target of RHO1 small GTP-binding protein is *PKC1*, a homolog of protein kinase C, which leads to activation of the MAP kinase cascade in *Saccharomyces cerevisiae*. EMBO J. **14:**5931–5938.
36. **Ono, T., T. Suzuki, Y. Anraku, and H. Iida.** 1994. The *MID2* gene encodes a putative integral membrane protein with a Ca(2+)-binding domain and shows mating pheromone-stimulated expression in *Saccharomyces cerevisiae*. Gene **151:**203–208.
37. **Orlean, P.** 1997. Biogenesis of yeast wall and surface components, p. 229–362. *In* J. R. Pringle, J. R. Broach, and E. W. Jones (ed.), The molecular and cellular biology of the yeast *Saccharomyces*—cell cycle and cell biology. Cold Spring Harbor Laboratory Press, Cold Spring Harbor, N.Y.
38. **Pagé, N., J. Sheraton, J. L. Brown, R. C. Stewart, and H. Bussey.** 1996. Identification of *ASK10* as a multicopy activator of Skn7p-dependent transcription of a *HIS3* reporter gene. Yeast **12:**267–272.
39. **Popolo, L., D. Gilardelli, P. Bonfante, and M. Vai.** 1997. Increase in chitin as an essential response to defects in assembly of cell wall polymers in the *ggp1*Δ mutant of *Saccharomyces cerevisiae*. J. Bacteriol. **179:**463–469.
40. **Ram, A. F., S. S. Brekelmans, L. J. Oehlen, and F. M. Klis.** 1995. Identification of two cell cycle regulated genes affecting the beta 1,3-glucan content of cell walls in *Saccharomyces cerevisiae*. FEBS Lett. **358:**165–170.
41. **Ram, A. F., J. C. Kapteyn, R. C. Montijn, L. H. Caro, J. E. Douwes, W. Baginsky, P. Mazur, H. van den Ende, and F. M. Klis.** 1998. Loss of the plasma membrane-bound protein Gas1p in *Saccharomyces cerevisiae* results in the release of β-1,3-glucan into the medium and induces a compensation mechanism to ensure cell wall integrity. J. Bacteriol. **180:**1418–1424.
42. **Roemer, T., and H. Bussey.** 1991. Yeast β-glucan synthesis: *KRE6* encodes a predicted type II membrane protein required for glucan synthesis *in vivo* and for glucan synthase activity *in vitro*. Proc. Natl. Acad. Sci. USA **88:**11295–11299.
43. **Roncero, C., and A. Duran.** 1985. Effect of calcofluor white and congo red on fungal wall morphogenesis: in vivo activation of chitin polymerization. J. Bacteriol. **170:**1950–1954.
44. **Schekman, R., and V. Brawley.** 1979. Localized deposition of chitin on the yeast cell surface in response to mating pheromone. Proc. Natl. Acad. Sci. USA **76:**645–649.
45. **Tanner, W., and L. Lehle.** 1987. Protein glycosylation in yeast. Biochim. Biophys. Acta **906:**81–99.
46. **Takeuchi, J., M. Okada, A. Toh-e, and Y. Kikuchi.** 1995. The *SMS1* gene encoding a serine-rich transmembrane protein suppresses the temperature sensitivity of *HTR1* disruptant in *Saccharomyces cerevisiae*. Biochim. Biophys. Acta **1260:**94–96.
47. **Verna, J., A. Lodder, K. Lee, A. Vagts, and R. Ballester.** 1997. A family of genes required for maintenance of cell wall integrity and for the stress response in *Saccharomyces cerevisiae*. Proc. Natl. Acad. Sci. USA **94:**13804–13809.
48. **Wach, A., A. Brachat, R. Pöhlmann, and P. Philippsen.** 1994. New heterologous modules for classical or PCR-based gene disruptions in *Saccharomyces cerevisiae*. Yeast **10:**1793–1808.
49. **Zarzov, P., C. Mazzoni, and C. Mann.** 1996. The *SLT2*(*MPK1*) MAP kinase is activated during periods of polarized cell growth in yeast. EMBO J. **83:**93–91.